Shift variance behavior for different sub-band coding systems, Biorthogonal, Orthogonal and Bspline wavelets

Gamal Fahmy

Electrical Engineering Dept., Assiut University, Egypt

Abstract: *Sub-band coding has long been utilized and adopted in different compression, coding and reconstruction techniques in most signal processing applications. It has wide applications in communications, bit rate codec's, sampling, and compression for images, videos and speech. However sub-band coding systems in general suffer from a certain amount of shift variance of the output reconstructed signal, due to the frequency overlap between different sub-bands in the analysis stage. This overlap is known as non-ideal anti-aliasing.*

In this paper we simplify the shift variance analysis of sub-band coding systems in general, and we present different metrics that have been reported in the literature to measure the bounds of shift variance for Perfect Reconstruction (PR) sub-band systems, we simplify its mathematical analysis and illustrate with graphs the reasons for these bounds and compare them. We apply these metrics on Biorthogonal, Orthogonal and Bspline wavelets and present the worst case scenario for different input signals in terms of shift variance for all these sub-band coding systems, both numerically and graphically. We finally compare the shift variance behavior for different sub-band PR systems for different types of input signals.

Keywords: Shift variance, Bspline, multirate system

1.   Introduction

Multirate systems employ by definition sampling rate conversion which introduces an amount of linear periodical shift variance (LPSV) in the output reconstructed signal [1-3], in spite of the fact that the adopted sub-band filters are linear shift invariant (LSI). This LPSV can be noticed in different applications such as block transform, fractional sampling rate converters, multirate filter banks, sub-band quantization, and motion estimation. Several approaches in the literature tried to reduce or prevent LPSV has adopted Complex wavelets [4], cycle spinning [5], and circular shifted wavelets [6]. In [7-9] several effects of shift variance, and some of its consequences like cyclostationarities on re-sampled data and images, were presented.

   In this paper we present a quantitative measure for shift variance in different sub-band coding systems. We derive the worst case scenario for the amount of shift introduced in the output reconstructed signal from different types of input signals (such as a narrow band input signal or a wide band one). We analyze different metrics for shift variance that has been reported in the literature [10] in a simplified form and we apply it on different PR sub-band coding systems that have different orthogonality characteristics (Biorthogonal, Orthogonal and Bspline wavelets). We selected Bspline wavelets to be included in our comparison as they are well known of being semi orthogonal, as they are orthogonal across different scales/channels, but not orthogonal within the same channel, in other words they are orthogonal across time shifts but not across time scale. We present an upper bound for shift variance for these systems mathematically and experimentally. Finally we discuss our results and provide a tradeoff analysis between different sub-band coding structures. We claim that our main contribution is presenting the shift variance metrics reported in [10-13] in a much simplified forms, as well as applying and comparing it on different sub-band systems.

   Section 2 analyzes different shift variance bounds and metrics for multirate sub-band coding systems in general. Section 3 presents the bounds on shift variance for two channel (2-CH) PR sub-band coding systems for either orthogonal or biorthogonal systems. Section 4 presents our own developed shift variance bounds on Bspline PR sub-band coding systems. Finally a comparative result analysis of different bounds of shift variance on Biorthogonal, Orthogonal and Bspline wavelets is presented in section 5. Discussion and Conclusion in section 6 & 7, respectively

2.   Shift variance for subband coding system

In this paper we will note the following, for a *M* band multirate filter bank, Fig.1, if the input signal is *s[n]*, and the output of *s[n]* is *y[n]*, then when the input signal is shifted by *m* samples so that the input is *s[n-m]* , the output is denoted by $x^m[n]$, while $y^m[n] = y[n-m]$. Hence for a system to be fully shift invariant $x^m[n]$ should be equal to $y^m[n]$. We denote $r^m[n] = x^m[n] - y^m[n]$. The residual energy for any band, which is the energy for the difference signal $r^m[n]$ for a given input *s[n]*, which is proportional to the amount of shift variance in the band, would be,

$$E_r[m] = \left\| r^m[z] \right\|_2^2 = \frac{1}{2\pi} \int_{-\pi}^{\pi} \left| R^m(e^{j\omega}) \right|^2 d\omega = \frac{1}{2\pi} \int_{-\pi/M}^{\pi/M} \left\| r_M^m(e^{j\omega}) \right\|_2^2 d\omega \qquad (1)$$

Where $r^m{}_M[z]$, which is the modulation vector for the difference signal $r^m[n]$, is

$$r_M^m(z) = X_M^m(z) - Y_M^m(z) = \frac{z^{-m}}{M} [g_M(z) h_M^T(z) D^{-m} - D^{-m} g_M(z) h_M^T(z)] s_M(z) = T(m,z) s_M(z) \quad (2)$$

Where $D \in C^{MxM}$ a diagonal matrix diag $[1, W, W^2 \ldots \ldots, W^{M-1}]$, Hence, $D^{-m} =$ diag $[1, W^{-m}, W^{-2m} \ldots \ldots, W^{-m(M-1)}]$

The norm of $r^m{}_M[z]$ would be

$$\left\| r_M^m(z) \right\|_2^2 = (r_M^m(z))^T \overline{r_M^m(z)} = s_M^*(z)T^*(m,z)T(m,z)s_M(z) = s_M^*(z)A(m,z)s_M(z) \qquad (3)$$

Where the matrices $T(m,z), A(m,z) \in C^{MxM}$. Thus the residual energy would be

$$E_r[m] = \frac{1}{2\pi}\int_{-\pi/M}^{\pi/M} s_M^*(z)A(m,z)s_M(z)d\omega \qquad (4)$$

In any subband coding system for a filter bank K, if the output $x^m[n]$ which is because of the shifted input $s[n-m]$ can be expressed as $x^m = K\circ\tau_m(s)$, where K , $\circ$ are the filter bank and the concatenation process, and τ_m is the shift operator. Then, the shifted output signal $y^m[n]$ can be expressed as $y^m = \tau_m\circ K(s)$. Hence for a the filter bank K to be fully shift variant, $[K,\tau_m] = K\circ\tau_m - \tau_m\circ K$ should be zero for any input. This last term $[K,\tau_m]$ is known as a commutator [10-13], and it should be proportional to the mean square error between $x^m[n]$ and $y^m[n]$. Thus, $E_r[m] = \left\| [K,\tau_m](s) \right\|_2^2 \qquad (5)$

  We note here that in any subband coding system channel, fig.2, even if the analysis and synthesis filters are fully shift invariant, the processing inside the band (decimators and interpolators) causes a certain amount of shift variance. Even though this analogy may seem strange, as for any band M the decimation and interpolation by factor M shouldn't lose any data and is completely reversible in a any PR system [3,14], but if we remember that there is an amount of overlap between different channels (overlap of frequency between High Pass and Low Pass filters in a 2-CH system) that causes this data alteration (shift variance), we justify why the PR system is shift variant.
Hence in an ideal scenario, where all analysis (or synthesis) filters are ideal with sharp transition and no overlap between the filters, there PR system would be fully shift invariant in spite of the processing in the band. This can be verified in the result section where we see that most amount of shift variance is at frequency overlap regions in the filter frequency response graph, fig. 3-10.
Since we are interested in finding the worst shift variance behavior for a PR system, the error energy $E_r[m]$ should be maximum, this will happen if the residual input signal is $\left\| s[n] \right\|_2 \le 1$ for any input. Hence because of eq. 1-5, [10-13], the max eigenvalue of the operator norm $\left\| r_M^m(z) \right\|_2^2$, would be the upper bound of $E_r[m]$, which is the worst case scenario for shift variance in a M band multirate filter bank channel. The upper bound of $E_r[m]$ is denoted $E[m]$, where $E[m] = \sup E_r[m]$ and sup stands for supremum which is the least upper bound.

Hence $\qquad \boldsymbol{E[m] = \left\| [K,\tau_m](s) \right\|_\infty^2 = \max \lambda_1(m, e^{j\omega})} \qquad (6)$

Example of shift variance in a subband PR system (2-CH)
For a single channel case of a 2-CH PR filter bank, D and T would be,

$$D^{-1} = \begin{bmatrix} 1 & 0 \\ 0 & -1 \end{bmatrix} \text{and } T_i(z) = z^{-1} \begin{bmatrix} 0 & -G_i(z)H_i(-z) \\ G_i(-z)H_i(z) & 0 \end{bmatrix} \qquad (7)$$

Resulting in

$$\lambda_{i1}(e^{j\omega}) = \max(\left| G_i(-e^{j\omega})H_i(e^{j\omega}) \right|^2, \left| G_i(e^{j\omega})H_i(-e^{j\omega}) \right|^2) \qquad (8)$$

,which is the max eigenvalue for channel i. For a 2-CH multi-rate system, the PR property would imply

$$s_M(z) = \frac{1}{2}(g_{0M}(z)h_{0M}(z)^T + g_{1M}(z)h_{1M}(z))s_M(z) \qquad (9)$$

where $G(z) = \begin{bmatrix} G_0(z) & G_1(z) \\ G_0(-z) & G_1(-z) \end{bmatrix}$ $H(z) = \begin{bmatrix} H_0(z) & H_0(z) \\ H_1(z) & H_1(z) \end{bmatrix}$. Hence, $G_0(z) = \dfrac{2H_1(-z)}{\det(H(z))}$ and $G_1(z) = \dfrac{2H_0(-z)}{\det(H(z))}$

So, $\lambda_{01}(e^{j\omega}) = \max(\dfrac{2H_1(e^{j\omega})H_0(e^{j\omega})}{\left| \det(H(-e^{j\omega})) \right|^2}, \dfrac{2H_1(-e^{j\omega})H_0(-e^{j\omega})}{\left| \det(H(e^{j\omega})) \right|^2})$ and $\lambda_{01}(e^{j\omega}) = \lambda_{11}(e^{j\omega})$ (10)

In the last equation, the 2 eigenvalues of the norm of the 2-CH system were equal, as it is a perfect reconstruction system. This would lead to the following equation

$$\left\| [K_0, \tau_1] \right\|_\infty = \left\| [K_1, \tau_1] \right\|_\infty \qquad (11)$$

Fig. 3-6 shows examples of the worst case scenario of shift variance in different 2-Ch PR systems, we also show the frequency response of the associated analysis filters. It can be easily noticed that the max amount of shift variance exists around the overlap area.

3.   Bounds of Shift variance for 2-CH orthogonal and biorthogonal systems

As orthogonal subband PR system are more restrictive by definition and nature [1,3,14] and they also have less overlap between the Low Pass and High Pass regions, it is normal to expect that they introduce an amount of shift variance that is less than biorthogonal ones.

Since the max amount of shift variance for a 2-CH PR system, as in eq. 10, is

$$\lambda_{01}(e^{j\omega}) = \max(\frac{2H_1(e^{j\omega})H_0(e^{j\omega})}{\left|\det(H(-e^{j\omega}))\right|^2}, \frac{2H_1(-e^{j\omega})H_0(-e^{j\omega})}{\left|\det(H(e^{j\omega}))\right|^2})$$

and since $\dfrac{2H_1(e^{j\omega})H_0(e^{j\omega})}{\left|\det(H(-e^{j\omega}))\right|^2}$ or $\dfrac{2H_1(-e^{j\omega})H_0(-e^{j\omega})}{\left|\det(H(e^{j\omega}))\right|^2}$ typically equals a value of 1 for orthogonal 2-CH PR systems

[3,14]. It can be easily proved that the max amount of shift variance for an orthogonal system would not exceed a value of 1 in a normalized frequency response graph, fig.3-6

For biorthogonal systems due to their more degrees of freedom nature, their maximum eigenvalue (commutator) would exceed the value of 1, fig.5-6. For bi-orthogonal 2-CH PR systems, the $\lambda_1(m, e^{j\omega})$ function has a maximum higher than that of unitary (orthogonal) filter banks and corresponds to worst case scenario for shift variance for this band. The areas under both curves $\lambda_1(m, e^{j\omega})$ and $\lambda_2(m, e^{j\omega})$ for the bi-orthogonal systems are equal, and their worst case shift variance frequency is not center at $\pi/2$, but around it. The higher the maximum value of the curve in fig.4, the more shift variance it has. Table 1, lists the $E_r[m]$ values for different 2-CH PR filter banks. It can be realized that the shift variance behavior for all orthogonal systems tends to be the same for different filter types, this also applies for biorthogonal filter banks. Hence we can conclude that the worst case scenario for shift variance is more dependent of the filter bank structure (orthogonal or bi-orthogonal) rather than the filter type. We can also see that the higher the order of the utilized filter, the less is the $\lambda_1(m, e^{j\omega})$ value for the same filter type, which means less shift variance, as the filter frequency response is more ideal with sharper transition (and less overlap).

Wide band Input signals

It can be seen in fig. 3-7, that the worst case scenario of shift variance or near maximizers, is a narrow band signal around the transition frequency. To complement this worst case shift variance behavior, and to capture more of the filter properties rather than properties of the filter banks structure, we can apply an additional bound for shift variance, under the assumption that the input signal for the subband PR system exhibit a given amplitude spectra. Similar to earlier work in [10-13], we will use a wide band model spectra as the input signal, like a signal with a flat spectrum

If we specify an amplitude spectrum $\left|S(e^{j\omega})\right| = \Phi(e^{j\omega})$ we would also be specifying absolute values of the entries of the modulation vector $s_M(e^{j\omega})$. Hence, from the weight function $\omega(e^{j\omega}) = \sum_{m=0}^{M-1}\left|\Phi(W^m e^{j\omega})\right|^2$ formed from the modulated versions $\Phi(e^{j\omega})$, we can define this wide band input signal additional measure of shift variance by

$$\tilde{E}_w[m] = \frac{1}{2\pi}\int_{-\pi/M}^{\pi/M}\lambda_1(m, e^{j\omega})w(e^{j\omega})d\omega \qquad (12)$$

Hence, for these types of signals, the worst case scenario for shift variance corresponds to a weighted integration of the max eigenvalue of the commutator, $\sqrt{\lambda_1(m, e^{j\omega})}$, rather than its peak height as eq. 1-5. Similarly to eq.6 & 12, this additional measure $\tilde{E}_w[m]$ is also is the same for both channels $\tilde{E}_w[m]$, as $\left\|[K, \tau_m](s)\right\|_2^2 = \tilde{E}_w[m]$

For a 2-CH PR filter bank, we would have: $\tilde{E}_w[1] = \left\|[K, \tau_1](s)\right\|_2^2$, for every signal s with $\left|S(e^{j\omega})\right| = \Phi(e^{j\omega})$. By choosing $\Phi(e^{j\omega})$ to be wide band, this would correspond to the additional measure of shift variance for wide band signals. This additional bound corresponds to the area under $\lambda_1(m, e^{j\omega})$ and would typically decrease with the increase of the filter length, which would imply less width of either of the 2 curves in fig.4-7.

Table 1 also lists the $\tilde{E}_w[m]$ values for the same orthogonal and biorthogonal PR system of the previous subsection. It can be seen that this additional shift variance measure is more dependent on the filter type, rather than the filter structure. It is also eliminated when there is no overlap in the frequency response between the analysis filters in different channels, as it represents the area of the overlap, while the previous narrow band shift variance measure $E_r[m]$ corresponds to the max

value in the overlap region. Hence, the wide band input shift variance measure $\tilde{E}_w[m]$ is a stronger measure than narrow band shift variance measure $E_r[m]$, as it assumes that the input signal has a wide band flat spectrum.

4.   Shift variance bounds on Bspline PR sub-band coding systems

The mth order Bspline function $B_m(t)$, has a finite support and equals zero at $t=0$,m, and is represented by a polynomial of order $m-1$ at the knots $1,2,..,m$. It satisfies the recurrence relation:

$$B_m(t) = \frac{t}{m-1} B_{m-1}(t) + \frac{m-t}{m-1} B_{m-1}(t-1) \tag{13}$$

$$\frac{\partial B_m(t)}{\partial t} = B_{m-1}(t) - B_{m-1}(t-1)$$

The mth order Bspline time domain equivalent function would imply

$$B_m(t) = B_1(t) * B_1(t) * \ldots * B_1(t) \qquad \longleftarrow --- \quad m\ times \quad \longrightarrow \tag{14}$$

$B_m(t)$ is also symmetric about $m/2$; i.e. $B_m(\dfrac{m}{2}+t) = B_m(\dfrac{m}{2}-t)$ $\tag{15}$

In [15], a Bspline based PR multi-scale representation was introduced and for a 2-CH system, as in fig.2, it was shown that the analysis and synthesis filters are:

$$H_0 = \frac{B_m(\omega)}{B_m(\omega/2)} = \frac{1}{2^m} \sum_{k=0}^{m} \binom{m}{k} z^{-k} = \left(\frac{1+z^{-1}}{2}\right)^m \qquad , z = e^{j\frac{\omega}{2}} \tag{16}$$

$$H_1 = -E(-z)\tilde{H}_0(-z), \quad E(z) = \sum_{k=1}^{2m-1} B_{2m}(k) z^{-(k-1)} \qquad F_0 = z\frac{E(z)}{E(z^2)} \tilde{H}_0(z) \quad and \quad F_1 = z^{-1}\frac{\tilde{H}_0(-z^{-1})}{E(z^2)} \tag{17}$$

As shown before the shift variance for a Bspline PR sub-band coding system, could be assessed by a single channel case for either H_0 & G_0 or H_1 & G_1, Fig.1.

Hence, the max eigenvalue for either channel in a Bspline based 2-CH PR system, would be:

$$\lambda_{11} = \frac{|H_0(z)H_1(-z)|^2}{|\det H(z)|^2} = \frac{(\frac{1+z^{-1}}{2})^m (\frac{1+(-z)^{-1}}{2})^m \sum_{k=1}^{2m-1} B_{2m}(k) z^{-k-1}}{|\det H(z)|^2} \tag{18}$$

Where m in this case represents the Bspline order used, rather than the PR channel index as in section 3. As shown in eq.18, the eigenvalue of the operator norm would depend on the Bspline order m. We note here that the area under the operator norm curve for either channel is the same for any Bspline order, as in the case of orthogonal and bi-orthogonal filters. We also note that the worst case behavior of shift variance for narrow band input signals would be represented in the peak of the operator norm and would be around $\pi/2$ as the biorthogonal one. The additional bound of shift variance which is for wide band input signals, would correspond to the area under the max eigenvalue curve.

5.   Result Analysis

We carried out extensive simulation tests to measure both metrics $E_r[m]$ and $\tilde{E}_w[m]$ for different types of orthogonal, Bi-orthogonal and Bspline PR filters banks. Table 1, compares the numerical values of them for all utilized filters banks. Fig.3-9, shows the maximum Eigen value for both channels λ_0 and λ_1 for the whole frequency band for different orthogonal, bi-orthogonal and Bsplined based systems. As proven in sections 2, 3, and 4, the worst case scenario for shift variance for narrow band signals for a Bspline based PR system, would correspond to the peak point in the curves, while the worst case scenario for shift variance for wide band input signals would correspond to the range of frequencies inside the curve.

6.   Discussion

It can be easily proven both experimentally and mathematically that the worst case scenario for narrow band input shift variance signal for orthogonal PR subband coding systems won't exceed the unity value for a normalized frequency response graph, fig. 3, as proven in eq.10. For bi-orthogonal systems this narrow band input shift variance signal gets higher than 1 due to the more overlap between the high and Low bands.

For the additional shift variance bound of wide band input signal, orthogonal PR systems in general has a less area under the curve and less $\tilde{E}_w[m]$ value, which implies that their shift variance behavior is much less compared to biorthogonal PR systems.

For different Bspline orders, (sometimes) the higher the B-spline order, the higher is the pulse at the worst case scenario frequency (which would imply more shift variance). This is unexpected due to the increased filter length, which is supposed to imply less shift variance. However, the interpolating nature of Bsplines that is not suited for narrow band signals [16] can justify for us this behavior, also the wide band input signal behavior, which is the area under the operator norm

curve, λ_0 or λ_1, can make this small increase eliminated. For higher B-spline orders, this width of the operator norm curve is smaller, (which would imply less shift variance). From analyzing fig 5-7, it can be realized that the amount of increase in the frequency peak at the worst case scenario for the error norm is negligible compared to the amount of reduction of the width of the curve, for different Bspline orders. Hence the higher the B-spline order for this 2-Ch PR multi-rate system, the more shift invariant it is. Bsplines are also more suitable for wideband spectrum input signals. We note here that the average number of taps for an analysis/synthesis filter was 14 for the cubic Bspline, 25 for the quadratic Bspline and 35 for the 5th order B-spline. Typically for an ideal shift invariant Bspline filter, $\tilde{E}_w[m]$ tends to go to zero, while $E_r[1]$ tends to be 1. This analogy has been verified experimentally as in fig 4-6; however it was not possible to prove mathematically, eq.18. The cubic B-spline (order 3) tends to outperform some of the well known orthogonal or bi-orthogonal filter banks in terms of $E_r[1]$ or $\tilde{E}_w[1]$ values. It is obvious from comparing fig.3-9, that Bspline decomposition filters exhibits much less shift variance for similar filters lengths of other structures. We note here that this improvement for shift variance behavior with a Bspline subband coding PR system in general, is mainly due to the nature of Bsplines that are semi orthogonal, as they are orthogonal across different scales/channels, but not within the same channel [17] (orthogonal across time shifts, but not across time scale). Hence the overlap between different channels is reduced than in similar bi-orthogonal filters bank systems. This justifies their shift variance behavior improvement, it can also be seen in the frequency response High Pass and Low Pass graphs, fig 8-10.

7.   Conclusion and Acknowledgement

In this paper we presented some of the most popular metrics for shift variance, previously reported in [10-13] in a clear manner. Mathematical proof as well experimental simulations are illustrated to prove the achieved results and the shift variance worst bounds for different input scenarios on different decomposition structures (i.e. orthogonal and biorthgonal systems). We also applied the proposed shift variance bounds on a Bspline 2-CH multirate PR systems. Our analysis and testing implied that a higher order Bspline would correspond to less shift variance and would have a larger impact in reducing the shift variance behavior than higher corresponding orders for other PR systems such as orthogonal or biorthogonal systems. The author would like to acknowledge the help received from Prof. Til Aach, RWTH Aachen University, for the extensive help and simulation code. This work is funded from the Alexander von Humboldt foundation, Germany

Reference

1.   R. E. Crochiere and L. R. Rabiner, Multirate Digital Signal Processing, Englewood Cliffs: Prentice-Hall, 1983.
2.   C. M. Loeffler and C. S. Burrus, "Optimal design of periodically time-varying and multirate digital filters," IEEE Transactions on Acoustics, Speech, and Signal Processing, vol. 32, no. 5, pp. 991–997, 1984.
3.   P. P. Vaidyanathan and S. K. Mitra, "Polyphase networks, block digital filtering, LPTV systems, and alias-free QMF banks: A unified approach based on pseudocirculants," IEEE Transactions on Acoustics, Speech, and Signal Processing, vol. 36, pp. 381–391, 1988.
4.   I. W. Selesnick, R. G. Baraniuk, and N. G. Kingsbury, "The dual-tree complex wavelet transform," IEEE Signal Processing Magazine, vol. November, pp. 123–151, 2005
5.   R. R. Coifman and D. L. Donoho, "Translation-invariant de-noising," in Wavelets and Statistics, A. Antoniades and G. Oppenheim, Eds. New York: Springer, 1995, pp. 125–150.
6.   R. Leonardi and A. Signoroni, "Cyclostationary error analysis and filter properties in a 3D wavelet coding framework," Signal Processing: Image Communication, vol. 21, pp. 653–675, 2006.
7.   S. Akkarakaran and P. P. Vaidyanathan, "Bifrequency and bispectrum maps: A new look at multirate systems with stochastic inputs," IEEE Transactions on Signal Processing, vol. 48, no. 3, pp. 723–736, 2000.
8.   V. P. Sathe and P. P. Vaidyanathan, "Effects of multirate systems on the statistical properties of random signals," IEEE Transactions on Signal Processing, vol. 41, no. 1, pp. 131–146, 1993.
9.   A. K. Soman and P. P. Vaidyanathan, "Coding gain in paraunitary analysis/synthesis systems," IEEE Transactions on Signal Processing, vol. 41, no. 5, pp. 1824–1835, 1993.
10.   T. Aach and H. Fuhr, "On Bounds of Shift Variance in Two-Channel Multirate Filter Banks", IEEE Transactions on Signal Processing, vol. 57, issue 11, pp. 4292-4303, 2009
11.   T. Aach and D. Kunz, "A lapped directional transform for spectral image analysis and its application to restoration and enhancement," Signal Processing, vol. 80, no. 11, pp. 2347–2364, 2000.
12.   T. Aach, "Comparative analysis of shift variance and cyclostationarity in multirate filterbanks," IEEE Transactions on Circuits and Systems–I: Regular Papers, vol. 54, no. 5, pp. 1077–1087, 2007.
13.   T. Aach and H. Fuhr, "Shift variance, cyclostationarity and expected shift variance in multirate LPSV systems" IEEE Statistical Signal Processing Workshop (SSP), pp. 781 – 784, June 2011
14.   Feng Fan, Ignace Bruyland, Weile Zhua, "Analysis/synthesis filter banks designed for subband video compression", Signal Processing Vol. 55 (1), Nov. 1996, Pages 117-122
15.   M. F. Fahmy, G. Fahmy and O. F. Fahmy, "B-splines Wavelets for Signal Denoising and Image Compression", Journal of Signal, Image and Video Processing, Springer London Volume 5, Issue 2 (2011), Page 141.
16.   M. Unser, A. Aldroubi and M. Eden," B-Spline signal processing: Part I- Theory", IEEE Transactions on Signal Processing, vol. 41, No. 2,pp.821-833, February 1993.

17. G. Fahmy and T. Aach, "Enhanced Bspline based compression performance for images", IEEE International conference on Acoustics, Speech and Signal Processing, ICASSP, Dallas, March 2010.

Table 1 Uniform bound $E(1)$ and $\tilde{E}_w(1)$

Filter	$E(1)$	$\tilde{E}_w(1)$
B-spline order 3 (Cubic)	1.0053	0.1274
B-spline order 4 (Quad)	1.0624	0.0905
B-spline order 5	1.0314	0.0662
Johnston QMF 16	0.9902	0.1265
Johnston QMF 8	1.0047	0.2696
Smith Barnwell 16	1.0000	0.1207
Smith Barnwell 8	1.0000	0.2230
Multiplierless 4	1.0000	0.4136
Multiplierless 6	1.0018	0.3126
Multiplierless 8	1.0000	0.2813
Haar	1.0000	0.5000
Daubechies 10	1.0000	0.1609
Daubechies 30	1.0000	0.0928
Coiflet-5	1.0000	0.1544
Symmlet-8	1.0000	0.1799
Bi-orthogonal 5-3	1.158	0.3906
Bi-orthogonal 6-10	1.0841	0.2712
Bi-orthogonal 9-7	1.0301	0.2678
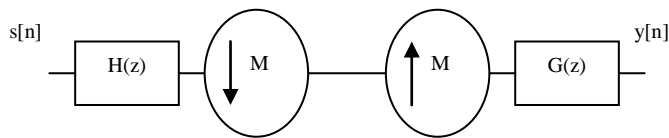
Fig. 1 Single Channel of a Multirate System
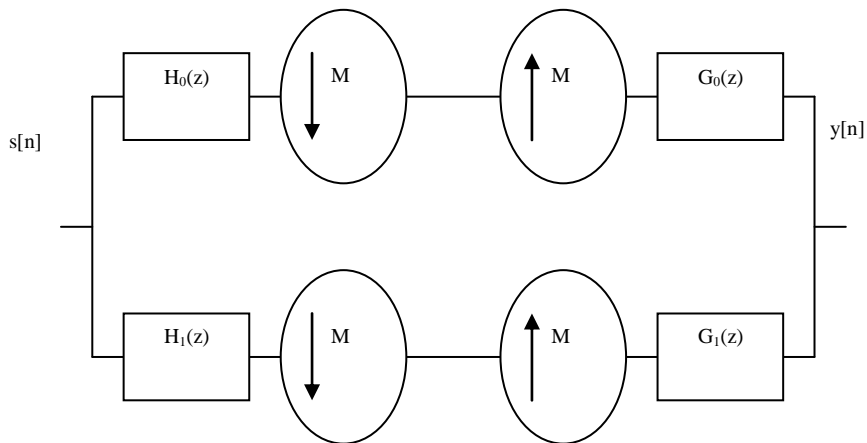
Fig. 2 2Ch PR Multirate System
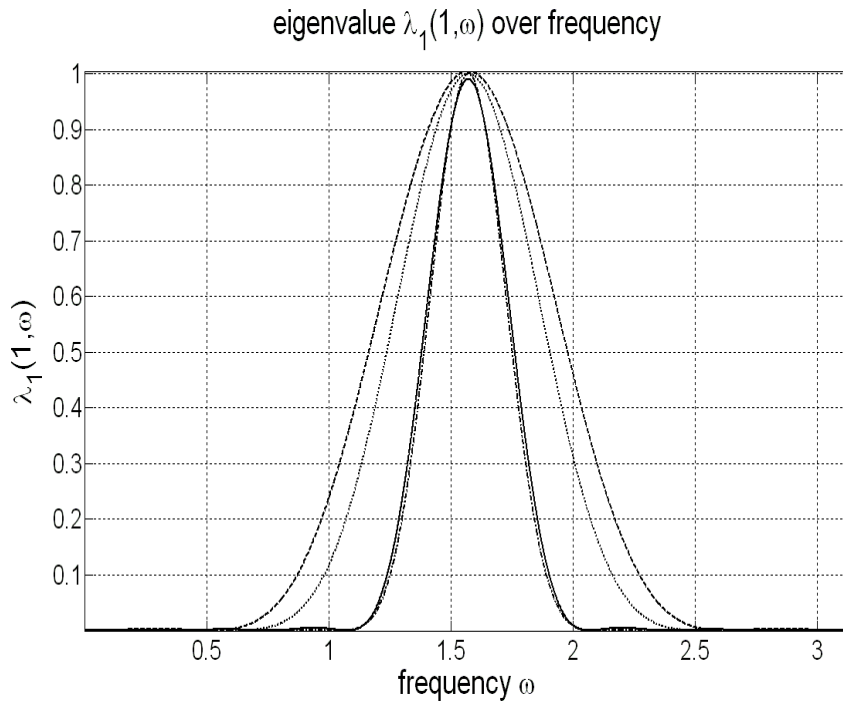
Fig. 3 max norm value (Eigen values) for different orthogonal filter banks, Johnston 16(solid), Johnston 8 (dashed line), Smith-Barnwell 16 & 8 (dotted-dotted dashed)
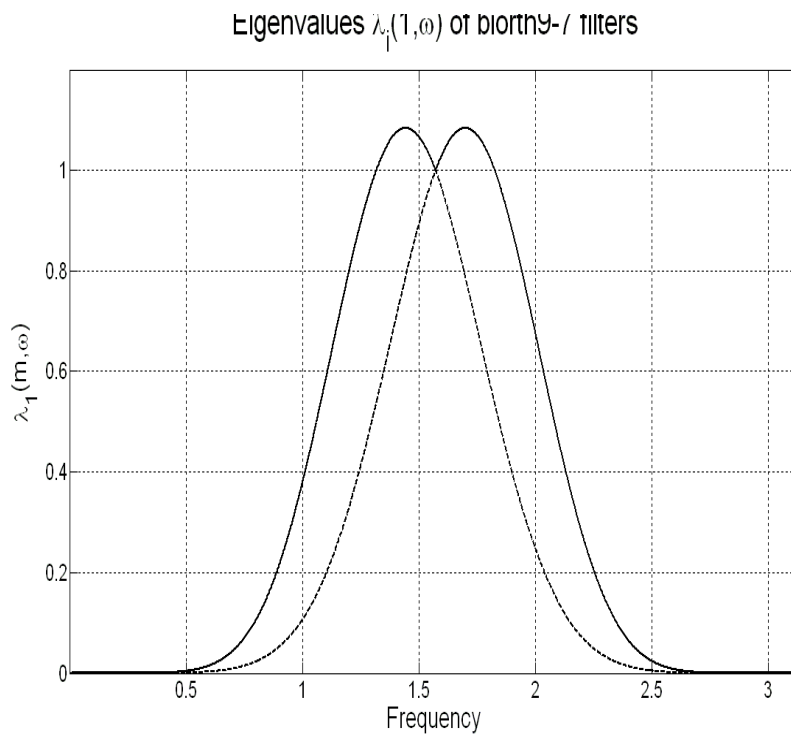

Fig. 4 max norm value (Eigen values) for Biorthogonal 9-7 Antonini filter banks
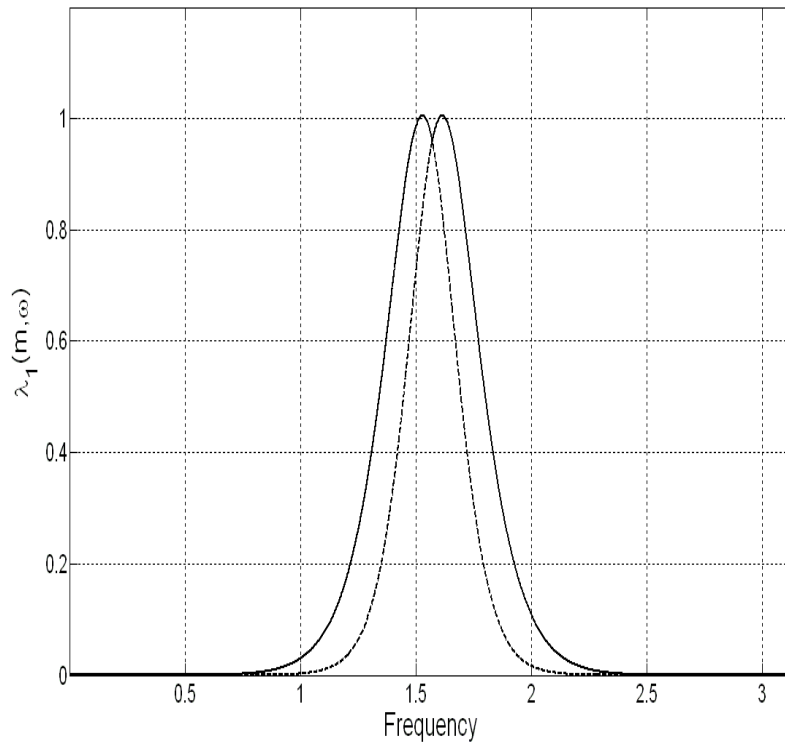
Eigenvalues $\lambda_i(1,\omega)$ of Cubic Bspline filters

Fig. 5 max norm for Cubic Bspline filter banks

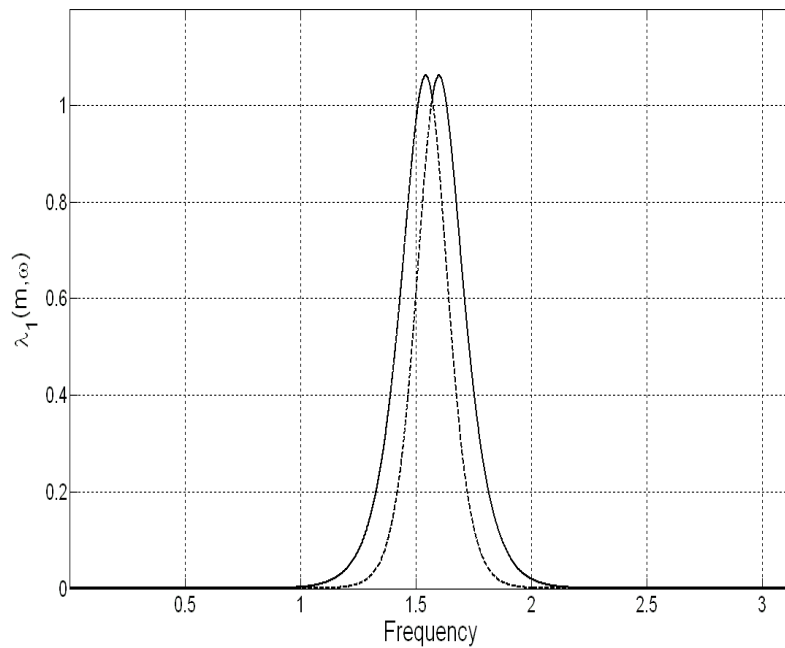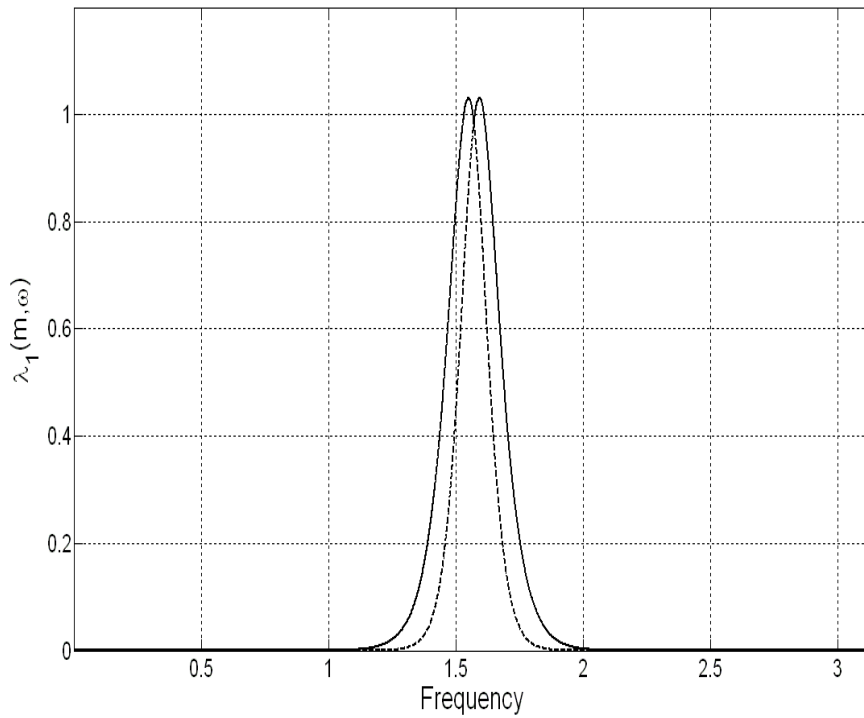Eigenvalues $\lambda_i(1,\omega)$ of Quadratic Bspline filters

Fig. 6 max norm for Quadratic Bspline filter banks
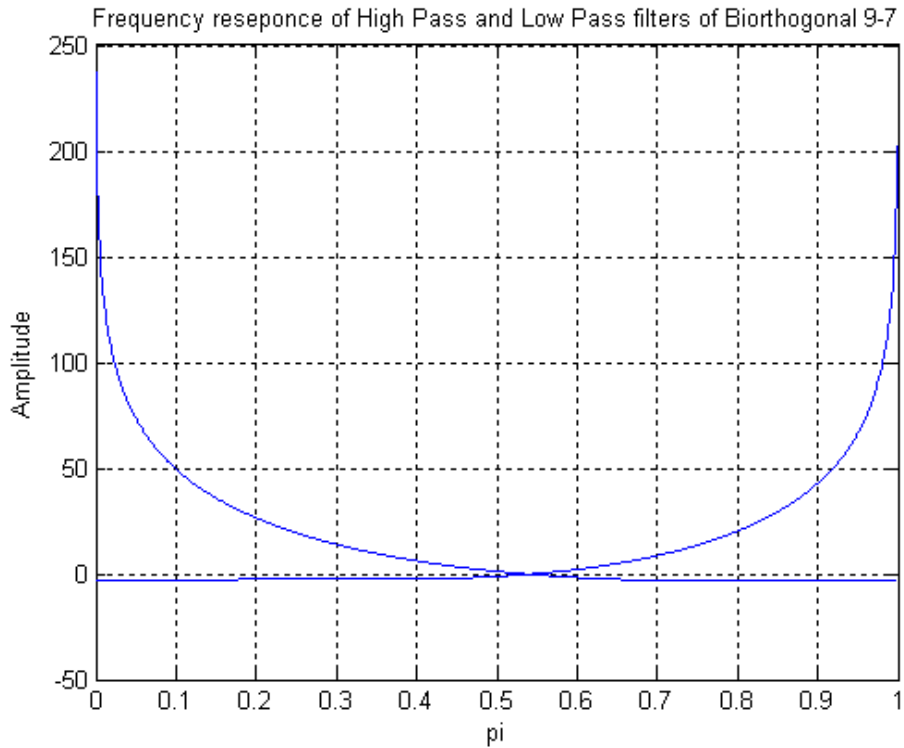
Fig. 7 max norm for 5th order Bspline filter banks

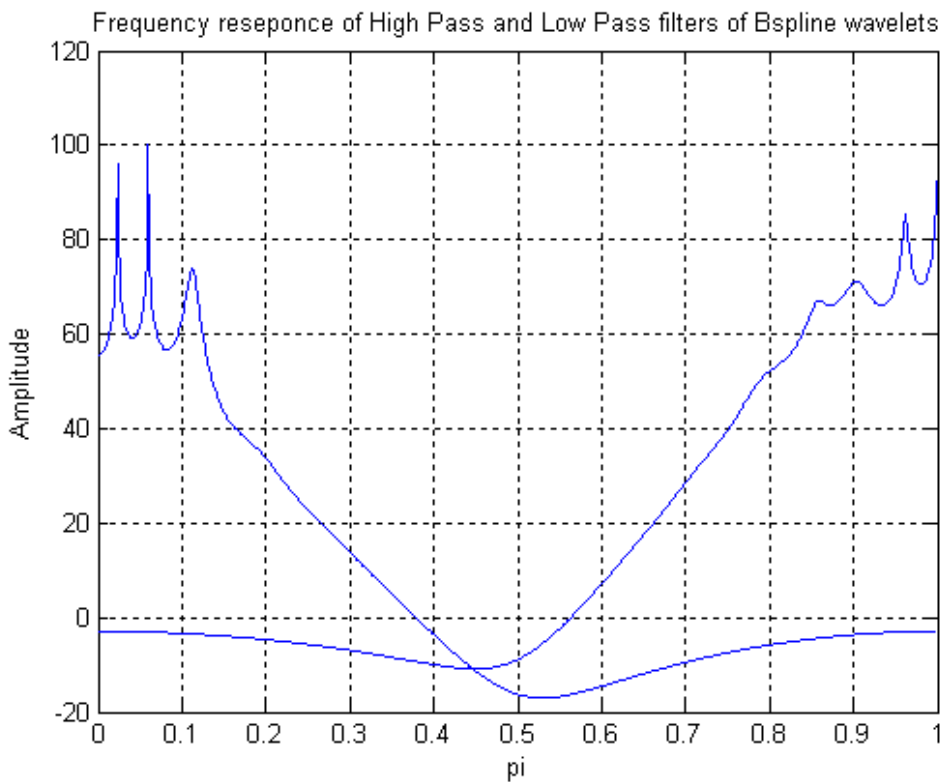Fig. 8 frequency responses overlap for Biorthogonal PR systems
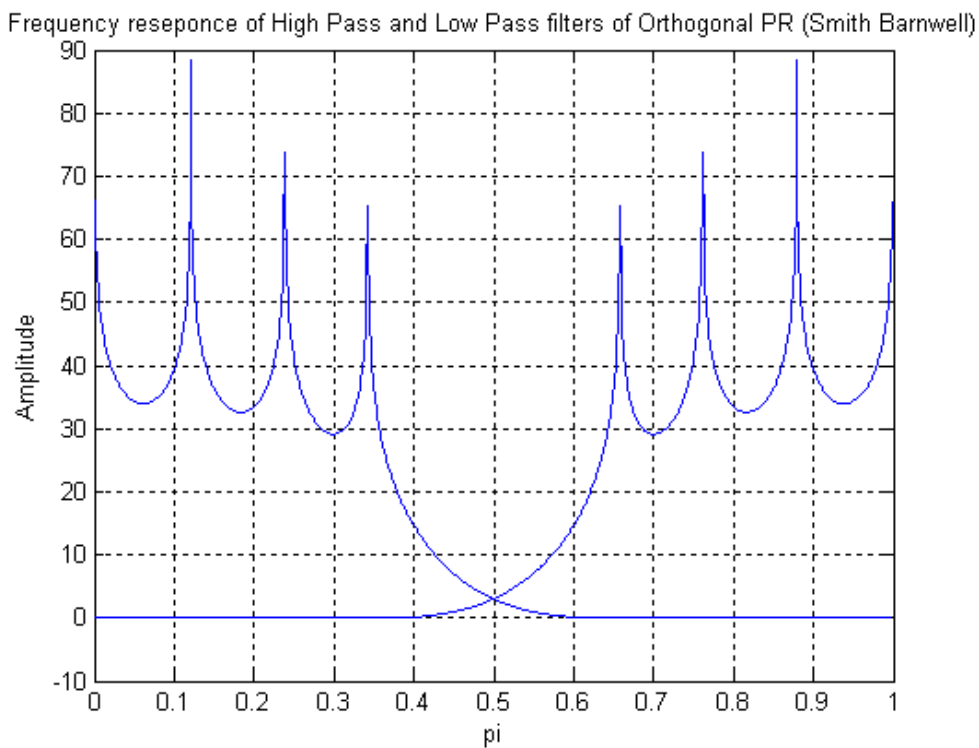
Fig. 9 frequency responses overlap for Bspline PR systems

Fig. 10 frequency responses overlap for Orthogonal PR systems